

## Hazelnut shell as a valuable bio-waste support for green synthesis of Ag NPs using *Origanum vulgare* leaf extract: Catalytic activity for reduction of methyl orange and Congo red

Bahar Khodadadi<sup>a,b,\*</sup>

<sup>a</sup>Department of Chemistry, Faculty of Science, University of Qom, Qom, Iran.

<sup>b</sup>Center of Environmental Researches, University of Qom, Qom, Iran.

Received 28 November 2016; received in revised form 12 March 2017; accepted 19 March 2017

### ABSTRACT

In this work the *Origanum vulgare* leaf extract was used to green synthesis of Ag nanoparticles (NPs) supported on Hazelnut shell as an environmentally benign support. The Ag NPs/Hazelnut shell as an effective catalyst was prepared through reduction of Ag<sup>+</sup> ions using *Origanum vulgare* leaf extract as the reducing and capping agent and Ag NPs immobilization on Hazelnut shell surface in the absence of any stabilizer or surfactant. According to FT-IR analysis, the hydroxyl groups of phenolics in *Origanum vulgare* leaf extract as bio-reductant agents are directly responsible for the reduction of Ag<sup>+</sup> ions and formation of Ag NPs. The as-prepared catalyst was characterized by Fourier transform infrared (FT-IR) and UV-Vis spectroscopy, field emission scanning electron microscopy (FESEM) equipped with an energy dispersive X-ray spectroscopy (EDS), X-ray diffraction analysis (XRD) and transmittance electron microscopy (TEM). The synthesized catalyst was used in the reduction of Methyl Orange (MO), and Congo Red (CR) at room temperature. The Ag/Hazelnut shell showed excellent catalytic activity in the reduction of these organic dyes. In addition, it was found that Ag/Hazelnut shell can be recovered and reused several times without significant loss of catalytic activity.

**Keywords:** Ag nanoparticles; Hazelnut shell; *Origanum vulgare*; NaBH<sub>4</sub>; Organic dyes.

### 1. Introduction

Azo dyes, which are widely used in the dying process in different industries such as ceramics, cosmetics, textile, paper, leather and food processing, are considered one of the major water pollutants in the environment [1-3]. Moreover, some of organic dyes such as organo-sulfur compound with high toxicity, strong corrosive material and also the volatile organic compound which it can be oxidized in the atmosphere to sulfuric acid (as main component of acid rain) [4,5]. Since organic dyes possess high resistance, conventional wastewater treatment methods including adsorption, reverse osmosis, or chemical coagulations are not sufficient and effective for their removal [6,7]. These methods solely transfer pollutants from the liquid to the solid phase. This causes secondary pollution and further treatment is required [8].

Nowadays, there is a growing need for more environmentally acceptable techniques for decolorization or detoxification of these compounds such as chemical reduction in the presence of metal nanoparticles (MNPs) [9]. MNPs can catalyze the reaction via facilitating electron transfer from the BH<sub>4</sub><sup>-</sup> donor to deal with the kinetic barrier. Large surface area to volume ratio of nanoparticles, which greatly enhances the interaction between catalysts and reactants, is their most significant and discrete property. However, the recovery and reusability of the metal catalysts is an important problem, which can be overcome using heterogeneous catalysts. Hitherto the development of a simple and green method for the preparation of heterogeneous catalysts has received a great deal of attention [9-12].

Silver nanoparticles (Ag NPs) have attracted a lot of attention due to their unique properties. Ag NPs are used in biosensors, antibacterial, antiviral and antifungal activities, drug delivery, and catalysis. Ag NPs are very stable, strong and have a longer shelf life

\*Corresponding author emails: khodadadi@qom.ac.ir; bkhodadadi98@yahoo.com

Tel.: +98 25 3210 3792; Fax: +98 25 3285 0953

compared to organic antimicrobial agents. Furthermore, having a high surface to volume ratio; Ag NPs can dramatically enhance the interaction between reactants and catalysts [13-15].

However, difficulties in their separation from reaction mixtures and agglomeration are some of the important drawbacks of Ag NPs. To prevent the agglomeration of MNPs and overcome the problems concerning their stability, separation, and recovery, immobilizing of the catalyst on the ideal support is needed. Up to now, several inorganic compounds such as zeolite that can serve as hosts to activate transition metal ions, graphene oxide, TiO<sub>2</sub> and Fe<sub>3</sub>O<sub>4</sub> have been used as supports for MNPs which dispersal of the catalyst particles on them [9-19]. Among various supports, biowastes are the best candidates because of their low cost and accessibility. Moreover, according to the literature, fruit kernel shell powder seems to be suitable for adsorption purposes due to its high surface area.

Hazelnut shell, which is a composite material mainly comprised of cellulose, hemicellulose, lignin and minor amounts of other organic compounds, is an agricultural by product obtained in large amounts. The main elements present in Hazelnut shell are carbon, hydrogen, oxygen, and nitrogen [20].

Various physical and chemical methods for the synthesis of silver nanoparticles including thermal reduction, metal vapor synthesis, radiation methods, microemulsion techniques, laser ablation, mechanical attrition, and chemical reduction have been reported [21-28]. However, high temperature and long reaction times, the use of expensive, hazardous and toxic capping agents or stabilizers, low purity, wide particle size distribution and complicated equipment are some of the disadvantages for these methods. Therefore, green methods for the synthesis of MNPs under mild conditions, avoiding organic solvents and toxic reagents are desired [29].

Recently, biosynthesis of MNPs using plant extracts as an environmentally benign compounds has received increasing attention due to high yields, cost effectiveness, environmental friendliness, elimination of organic solvents, easy work up and scale up [30-33]. We believe, biosynthesis of Ag NPs supported on the Hazelnut shell surface using *Origanum vulgare* extract has not been reported till now.

*Origanum vulgare* (Fig. 1) is a natural and aromatic plant of the Mediterranean flora with more than 40 species, which is traditionally used worldwide for its medicinal applications including respiratory disorders, indigestion, dental caries, rheumatoid arthritis and urinary tract disorders.



**Fig. 1.** Image of *Origanum vulgare*.

However, the biological activity of *Origanum vulgare* strongly depends on its composition. The analysis of *Origanum vulgare* shows that it has different phenol compounds with proved antioxidant and antimicrobial properties. In fact, studies on the *Origanum vulgare* leaf extract revealed the presence of phenolic compounds especially flavonoids to which are attributed many of the antioxidant properties, due to supporting a green reducing media through their hydrogen donation ability and structural requirements considered to be essential for effective radical scavenging and production of nanoparticles [34-36]. Of course it should be added that any other species containing the antioxidant phenolics can be used for biosynthesis of the nanoparticles but what is important here is the type and category of the antioxidant phytochemicals because beside those reducing effect to produce the nanoparticles they adsorb on nano surface and determine the size, shape and morphology of the biosynthesized nanoparticles, furthermore, they enhance the ability of catalyst and also prevent the agglomeration process and deforming the nanosurface.

The synthesis of MNPs using plant extracts has been recently reported. Herein, an environmentally friendly, clean and non-toxic method is reported for the first time for the green synthesis of Ag NPs/Hazelnut shell using *Origanum vulgare* leaf extracts in the absence of any stabilizer or surfactant. The catalytic activity of Ag NPs/Hazelnut shell in the reduction of MO and CR using aqueous NaBH<sub>4</sub> has also been studied.

## 2. Experimental

### 2.1. Instruments and reagents

Highly pure chemical reagents were obtained from Merck and Aldrich Chemical Companies. Characterization of the products was carried out by

comparison of their physical and spectral data with those of authentic samples. A Nicolet 370 FT-IR spectrophotometer (Thermo Nicolet, USA) was used to record FT-IR spectra using pressed KBr pellets. A Philips model X'Pert Pro diffractometer was used to carry out X-ray Diffraction (XRD) measurements using Ag K $\alpha$  radiation ( $\lambda=1.5418\text{\AA}$ ) at a scanning rate of 2 °/min in the 2 $\theta$  range of 10-80°. A Shimadzu UV-2500 double beam spectrophotometer was used to record UV-Visible spectra in the wavelength range of 200-700 nm. The sample shapes and sizes were identified by Transmission Electron Microscopy (TEM) using a Zeiss-EM10C operating at an accelerating voltage of 80 kV. A Cam scan MV2300 was used to perform Scanning Electron Microscopy (SEM). EDS (Energy Dispersive X-ray Spectroscopy) performed in SEM was used to determine the measured chemical composition of the prepared nanostructures.

## 2.2. Preparation of extract of the leaves of *Origanum vulgare*

20 g of *Origanum vulgare* dried leaf powder were extracted by heating in 100 mL of a 70% (V/V) ethanol solution at 70°C for 30 min. After cooling the mixture to room temperature, the aqueous extract of *Achillea millefolium* *Origanum vulgare* was centrifuged at 6500 rpm and supernatant separated by filtration.

## 2.3. Green synthesis of silver nanoparticles using *Origanum vulgare* leaf extract

In a 250 mL conical flask, 5 mL of a solution of AgNO<sub>3</sub> (2.5 mM) were mixed with 50 mL of *Origanum vulgare* leaf extract under vigorous shaking until the color of the mixture gradually changed to dark during 30 min, indicating the formation of Ag nanoparticles (as monitored by UV-Vis and FT-IR spectra of the solution). On completion of silver ion (Ag<sup>+</sup>) reduction to silver (Ag<sup>0</sup>), the NP solution was centrifuged at 6500 rpm for 30 min to completely precipitate Ag NPs. The obtained precipitate was then washed several times with distilled water and one time with ethanol and air dried for 24 h at 50°C in an oven.

## 2.4. Preparation of Ag/Hazelnut shell nanocomposite

In a 250 mL conical flask, 1.0 g of dried micro powdered Hazelnut shell was mixed with 0.4 g of AgNO<sub>3</sub> and 50 mL of the *Origanum vulgare* leaf extract. The mixture was then heated at 70 °C under vigorous shaking for 2 h until the color of the mixture gradually changed, indicating the formation of Ag/Hazelnut shell nanocomposite (as monitored by UV-Vis) and the product was subsequently filtered. Ag/Hazelnut shell nanocomposite was centrifuged at

6500 rpm for 30 min. The obtained precipitate was then washed several times with distilled water and one time with ethanol and air dried for 24 h at 50°C in an oven.

## 2.5. MO catalytic reduction

In a typical experiment, different amounts of Ag/Hazelnut shell nanocomposite were added to an aqueous solution containing MO ( $3.0 \times 10^{-5}$  M, 25 mL) and freshly prepared aqueous NaBH<sub>4</sub> solution ( $5.3 \times 10^{-3}$  M, 25 mL). The mixture was stirred until the solution color vanished, which indicated the complete degradation of the dye at room temperature. The change of the absorption peak at 465 nm was recorded to reflect the successive information about the reduction of MO. After completion of the reaction, the catalyst was separated from the reaction mixture by centrifugation, washed with doubly distilled water and then dried for the next cycle.

## 2.6. CR catalytic reduction

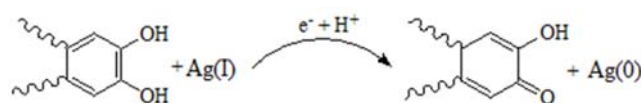
In a typical experiment, different amounts of the catalyst was added to an aqueous solution containing CR ( $1.44 \times 10^{-5}$  M, 25 mL) and freshly prepared aqueous NaBH<sub>4</sub> solution ( $5.3 \times 10^{-3}$  M, 25 mL). The mixture was stirred until the solution color vanished at room temperature. The change of the absorption peak at 493 nm was recorded to reflect the successive information about the reduction of CR. After completion of the reaction, the catalyst was separated from the reaction mixture by centrifugation, washed with doubly distilled water and then dried for the next cycle.

## 3. Results and Discussion

Ag/Hazelnut shell nanocomposite was synthesized via an efficient, simple, non-toxic, eco-friendly and inexpensive method in this work using *Origanum vulgare* leaf extract, which functions both as reducing and stabilizing agents (Scheme 1).

### 3.1. Characterization of *Origanum vulgare* leaf extract and Ag NPs

The presence of polyphenolics as antioxidant sources in the green synthesis of nanoparticles was evaluated by FT-IR and UV-Vis analyses of *Origanum vulgare* leaf extract.



**Scheme 1.** Mechanism for green synthesis of Ag NPs using *Origanum vulgare* leaf extract.

The UV-Vis spectrum of *Origanum vulgare* leaf extract (Fig. 2a) shows bands at around 330 nm, related to the benzoyl system and  $\pi \rightarrow \pi^*$  or  $n \rightarrow \pi^*$  transitions. These absorbent bands demonstrate the presence of polyphenolics as antioxidant sources for green synthesis of nanoparticles. Moreover, the absorption at 270 nm is due to the absorbance of ring related to the benzoyl system and  $\pi \rightarrow \pi^*$  transitions and demonstrates the presence of phenolics [28].

The UV-Vis spectrum of green synthesized Ag NPs using *Origanum vulgare* leaf extract (Fig. 2b) showed a maximum absorbance at with  $\lambda_{\text{max}}$  ranging 440 nm, indicating the formation of Ag NPs, as characterized by UV-Vis spectrum. This absorbance can be assigned to the surface plasmon absorption of silver nanoparticles [26,28,29].

FT-IR spectrum of *Origanum vulgare* leaf extract (Fig. 3a) shows some peaks at 3500-3100, 1670, 1455, 1270-1050  $\text{cm}^{-1}$ , which represent free OH in molecule and OH group forming hydrogen bonds, carbonyl group (C=O), stretching C=C aromatic ring and C-OH stretching vibrations, respectively. Due to the presence of these functional groups inside the structure of polyphenolics, the spectrum demonstrates the presence of phenolics in the *Origanum vulgare* leaf extracts.

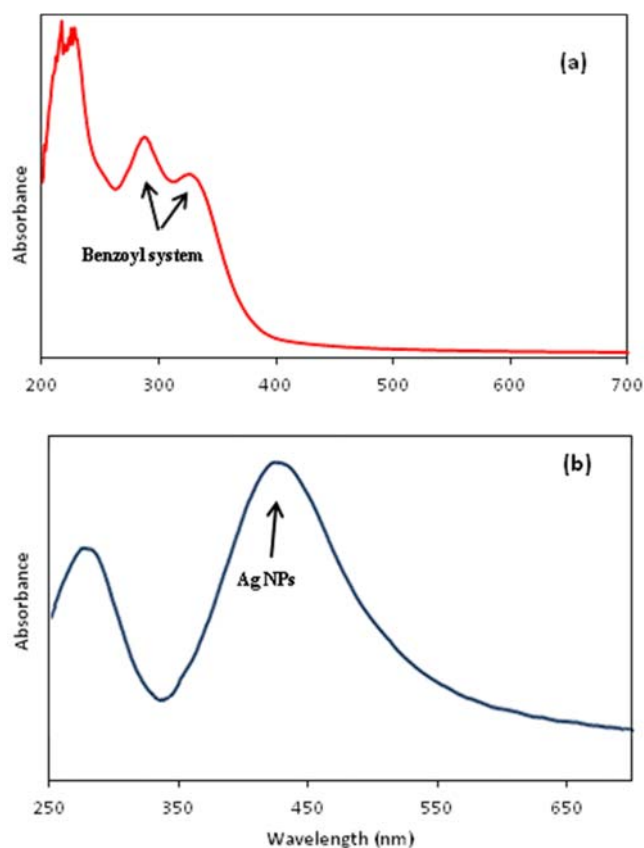


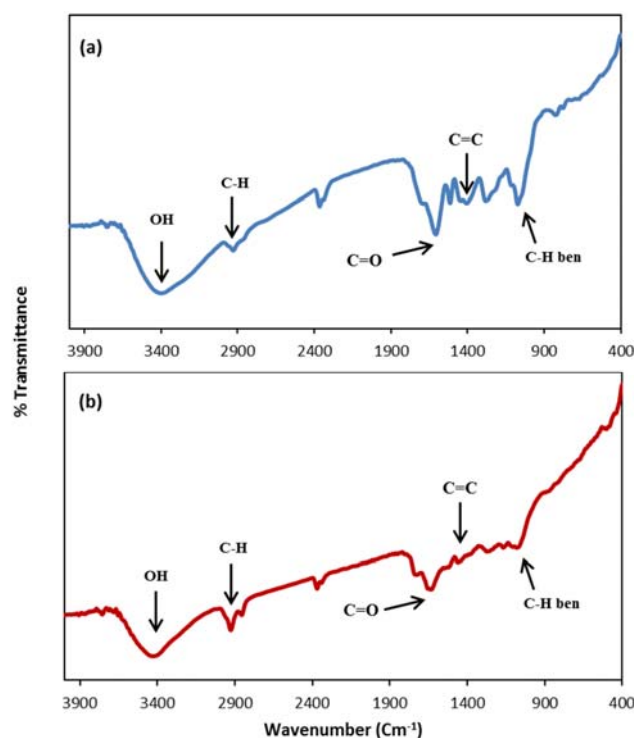
**Fig. 2.** (a) UV-Vis spectra of *Origanum vulgare* leaf extract, (b) Synthesized Ag NPs using *Origanum vulgare* leaf extract.

Furthermore, the FT-IR of Ag NPs shows demonstrative differences in the shape and location of signals, indicating the interaction between  $\text{AgNO}_3$  and involved sites of phytochemicals for production of nanoparticles (Fig. 3b). The shift of peaks at 3500 to 3100, 1685, 1465, 12850 and 1100  $\text{cm}^{-1}$  represent the OH functional groups, carbonyl group (C=O), stretching C=C aromatic ring and C-OH stretching vibrations, respectively. Polyphenolics can be adsorbed on the surface of metal nanoparticles, possibly by interaction through interaction of  $\pi$ -electrons in the absence of other strong ligating agents [12,28].

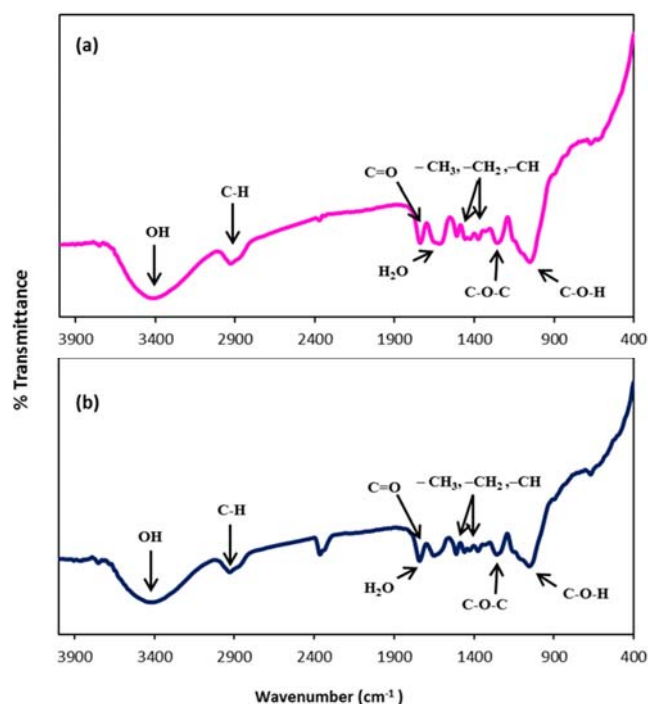
### 3.2. Characterization of Hazelnut shell and Ag/Hazelnut shell nanocomposite

Fig. 4 illustrates the FT-IR spectra of Hazelnut shell and Ag/Hazelnut shell nanocomposite. Typical functional groups for Hazelnut shell are observed in FT-IR spectra.

The broad peak observed at 3500 to 3100  $\text{cm}^{-1}$  in the spectra of the Hazelnut shell and Ag/Hazelnut shell nanocomposite corresponds to free OH in molecule and OH group forming hydrogen bonds of stretching groups of macromolecular association. The absorption band at 2920  $\text{cm}^{-1}$  is related to the C-H stretching vibrations. Another small absorption peak at 1620  $\text{cm}^{-1}$  can be associated with the bending vibrations of  $\text{H}_2\text{O}$  molecules.



**Fig. 3.** (a) FT-IR spectra of *Origanum vulgare* leaf extract, (b) Synthesized Ag NPs using *Origanum vulgare* leaf extract.



**Fig. 4.** (a) FT-IR spectra of Hazelnut shell, (b) Ag/Hazelnut shell nanocomposite.

In addition, the absorption bands at 1360 and 1470  $\text{cm}^{-1}$  indicate the presence of  $-\text{CH}_3$ ,  $-\text{CH}_2$  and  $-\text{CH}$ , which are characteristic of alkane groups, cellulose, hemicellulose, and lignin. In addition, the absorbance 1740  $\text{cm}^{-1}$  is due to the  $\text{C}=\text{O}$  stretching vibrations. Moreover, the peaks at 1245 and 1050  $\text{cm}^{-1}$  can be attributed to the  $\text{C}-\text{O}-\text{C}$  and  $\text{C}-\text{O}-\text{H}$  functional groups in the compounds [37-41]. In comparison with Hazelnut shell, the FT-IR analysis of Ag/Hazelnut shell nanocomposite confirms that there are no changes in functional groups after the immobilization of Ag NPs on Hazelnut shell.

The crystalline nature of the Hazelnut shell and Ag/Hazelnut shell nanocomposite was confirmed by XRD and the results are illustrated in Fig. 5. Obviously, cellulose is the main component of Hazelnut shell and according to the literature, the peak at  $2\theta$  around  $22^\circ$  is an evidence of cellulose, which is in good agreement with the XRD result [42,43]. Moreover, the XRD peaks at  $38.73^\circ$ ,  $44.26^\circ$ ,  $64.59^\circ$ , and  $78.12^\circ$  were assigned to the Ag NPs, JCPDS no. 04-0783) [21], which exhibited face centered cubic (FCC) structure for the metallic silver NPs immobilized on the surface of Hazelnut shell without impurities like silver oxide ( $\text{Ag}_2\text{O}$  or  $\text{AgO}$ ) [13,26].

The microstructure information of the samples was investigated by field emission scanning electron microscopy (FESEM).

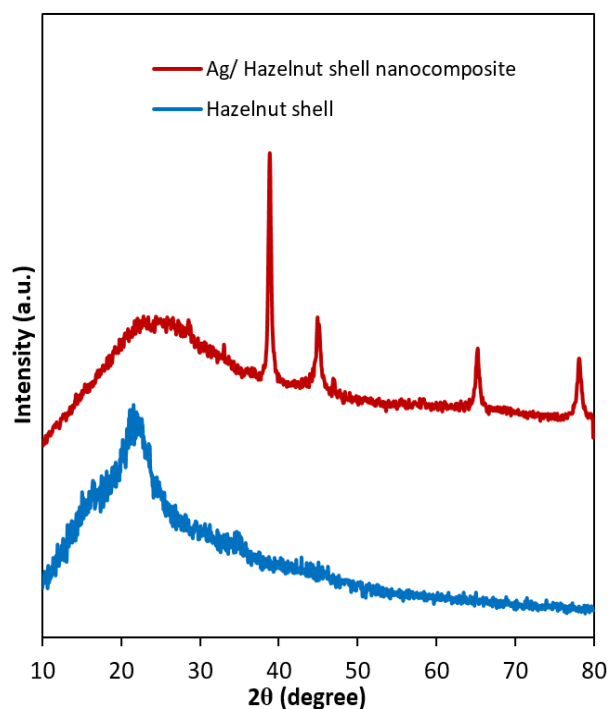


**Fig. 5.** XRD pattern of Hazelnut shell and Ag/Hazelnut shell nanocomposite.

Fig. 6 shows the FESEM images of Hazelnut shell and Ag/Hazelnut shell nanocomposite. It can be easily observed in Fig. 6 that Hazelnut shell and Ag/Hazelnut shell nanocomposite show spherical morphology with diameters of less than 30 nm. It is clearly observed that the Ag NPs are immobilized on the Hazelnut shell surface, which displays a good combination between support and Ag NPs.

EDS spectroscopy was used to determine the elemental composition of Ag/Hazelnut shell nanocomposite (Fig. 7). EDS spectroscopy verified the presence of C, N, O, and Ag elements in the Ag/Hazelnut shell nanocomposite.

Furthermore, the morphology and size of Ag/Hazelnut shell nanocomposite were studied by Transmission Electron Microscopy (TEM). Fig. 8 shows TEM images of Ag/Hazelnut shell nanocomposite. The Ag NPs are very small with a narrow size distribution. The TEM micrographs show that the Ag NPs are spherical with an average diameter of about 5 nm.

### 3.3. Evaluation of the catalytic activity of Ag/Hazelnut shell through the reduction of MO and CR

Having characterized the catalysts, the catalytic activity of the Ag/Hazelnut shell nanocomposite was examined in the reduction of MO and CR in water at room temperature. The progress of the reaction was monitored by recording the absorption spectra as a function of time.

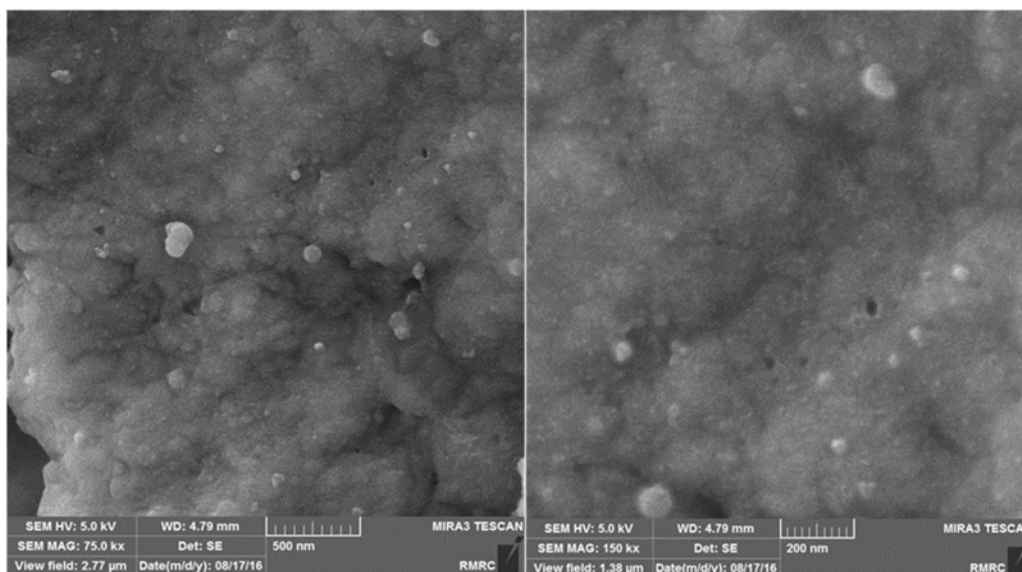


Fig. 6. FE-SEM image Ag/Hazelnut shell nanocomposite.

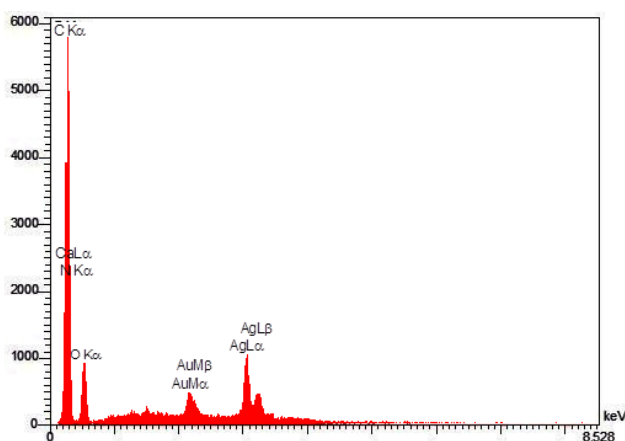


Fig. 7. EDS spectrum of Ag/Hazelnut shell nanocomposite.

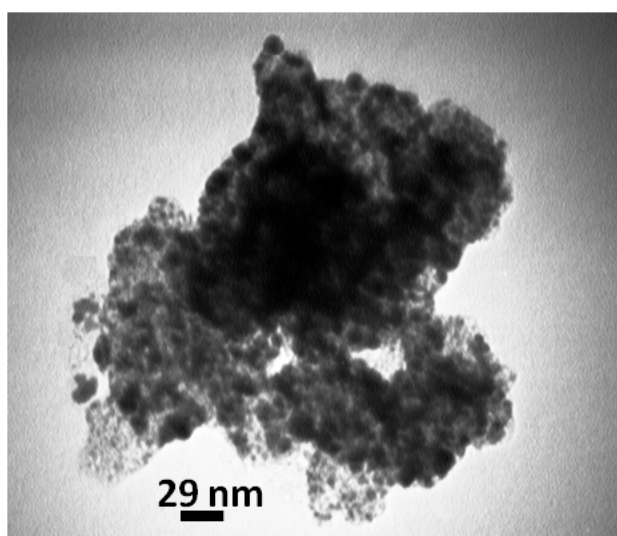


Fig. 8. TEM image of Ag/Hazelnut shell nanocomposite.

Firstly, the reduction of 10 ppm and CR dyes (25 mL) using 10 mg of Hazelnut shell in the presence of 25 mL of  $\text{NaBH}_4$  ( $5.3 \times 10^{-3}$  M) was examined. However, after 150 min, no changes were observed. Constant amounts of  $\text{NaBH}_4$  and different amounts of catalyst were then applied in the catalytic reduction of MO or CR dyes (Table 1).

The catalytic reduction of dyes with an appropriate amount of  $\text{NaBH}_4$  has often been used as a model reaction to evaluate the catalytic performance of metal nanoparticles. In principle, the choice of dye is based on the following factors: first, the reduction of all dyes is thermodynamically favorable but not kinetically; second, the dyes have different colors in their oxidized and reduced states, and their major spectral bands do not overlap with the plasmon bond of silver. In this step, the Ag- Hazelnut shell can act as an electron relay system. The metal nanoparticles start the catalytic reduction by relaying electrons from the donor  $\text{BH}_4^-$  to the acceptor dye molecules, where the Ag - Hazelnut shell accepts electrons from  $\text{BH}_4^-$  ions and conveys them to the dyes. At the early stage, dye molecules could easily transport to the Ag surface because of the strong adsorption and reduction ability of the Ag- Hazelnut shell. During this process, the  $\text{H}_2$  generated can cause the convection of the water and the nanoparticles, and remove the alteration products, thus keeping the surface fresh and maintaining the high reactivity of the nanoparticles. The results indicate that the absence of Ag- Hazelnut shell or  $\text{NaBH}_4^-$  did not produce fading and bleaching of the color for MO and CR. In the presence of  $\text{NaBH}_4^-$ , the addition of the Ag- Hazelnut shell can cause the fast reduction of these

dyes, while the addition of precursor Hazelnut shell demonstrates no catalytic effect on the reduction of the dyes. All the facts suggest that only  $\text{NaBH}_4$  is used as a reducing agent [12,44,45].

It seems that the adsorption of  $\text{NaBH}_4$  on the surface of catalyst and formation of metal hydride, adsorption of MO or CR on the surface of catalyst, and reduction of MO or CR and desorption in order to create free space for the continuing of reaction was take place. The mechanism of the catalytic reduction degradation of dyes with Ag/Hazelnut shell nanocomposite is shown in Scheme 2 [44,45].

As observed in UV-Vis spectra, aqueous solutions of MO and CR exhibit peaks at  $\lambda_{\text{max}}$  466 and 493 nm, which disappear when the reduction of dyes is complete. According to Fig. 9, 10 and data given in Table 1, as the best result, reduction of MO and CR using 10.0 mg of Ag/Hazelnut shell nanocomposite was complete within 55, 60 and 49 s, respectively.

Completion time for the reduction of MO and CR using Ag NPs and hazelnut shell and without any catalyst is given in Table 2. According to these results, it can be concluded that, hazelnut shell as a support could be employed successfully to decreases Ag NPs agglomeration and increases catalyst surface area.

### 3.4. Catalyst recyclability

The reusability of the heterogeneous catalysts, which makes them useful for industrial applications, is one of their advantages. Ag/Hazelnut shell nanocomposite catalyst can be easily removed from the reaction mixture by centrifugation and washing several times with distilled water for the successive reactions. The catalyst thus recovered was recycled five times for 100% dye reduction. The high stability and turnover of catalyst under operating conditions is demonstrated by its reusability. Little loss of catalytic activity was observed after the 5<sup>th</sup> cycle.

## 4. Conclusion

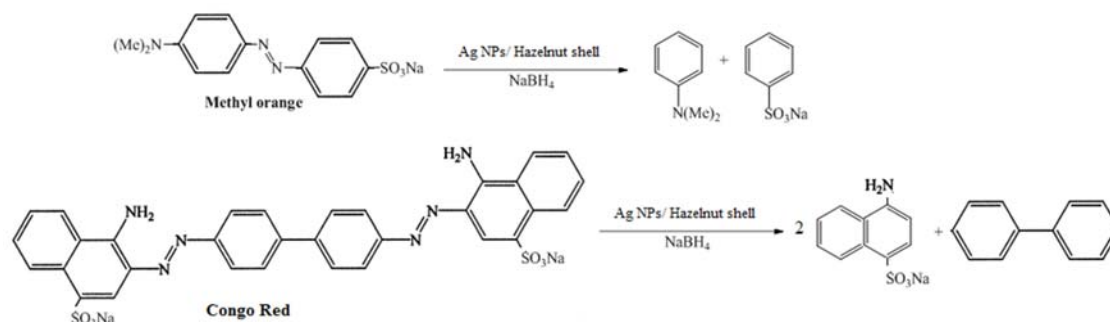
In conclusion, an environmentally friendly method was used in the synthesis of AgNPs and Ag/Hazelnut shell nanocomposites using Origanum vulgare leaf extract. The advantages of this method include the application of plant extract as an economic and effective alternative, low cost, cleanliness, non-toxicity and environmental friendliness of the precursor, absence of toxic reagents or surfactant templates and simplicity. SEM, XRD, EDS, FT-IR and UV-Vis spectroscopic techniques were used to characterize the synthetic Ag NPs and Ag/Hazelnut shell nanocomposite. Ag/Hazelnut shell nanocomposite catalytic activity in the reduction of MO and CR using aqueous  $\text{NaBH}_4$  at ambient temperature has also been studied. Ag/Hazelnut shell nanocomposite has desirable catalytic activity according to the experimental results in this study. In addition, the catalyst can be recycled for at least five times in the reduction of MO and CR with almost no loss of catalytic activity.

## Acknowledgements

We gratefully acknowledge the Iranian Nano Council and the University of Qom for the support of this work.

## References

- [1] Z. Han, L. Ren, Z. Cui, C. Chen, H. Pan, J. Chen, Appl. Catal. B 126 (2012) 298-305.
- [2] H.Y. Zhu, L. Xiao, R. Jiang, G.M. Zeng, L. Liu, Chem. Eng. J. 172 (2011) 746-753.
- [3] R. Saravanan, V.K. Gupta, T. Prakash, V. Narayanan, A. Stephen, J. Mol. Liq. 178 (2013) 88- 93.
- [4] H.R. Pouretdal, M. Ahmadi, Iran. J. Catal. 3 (2013) 149-155.
- [5] A. Nezamzadeh-Ejhih, Z. Banan, Iran. J. Catal. 2 (2012) 79-83.
- [6] T.J. Whang, M.T. Hsieh, H.H. Chen, Appl. Surf. Sci. 258 (2012) 2796-2801.
- [7] U. Kurtan, A. Baykal, H. Sozeri, J. Inorg. Organomet. Polym. 25 (2015) 921-929.



**Scheme 2.** Mechanism of the catalytic reduction and degradation of dyes with Ag/Hazelnut shell nanocomposite.

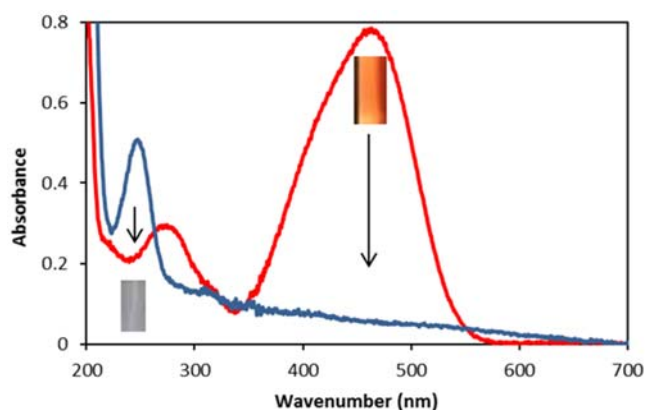


**Fig. 9.** The UV-Vis spectra of MO aqueous solution in the presence of Ag/Hazelnut shell nanocomposite.

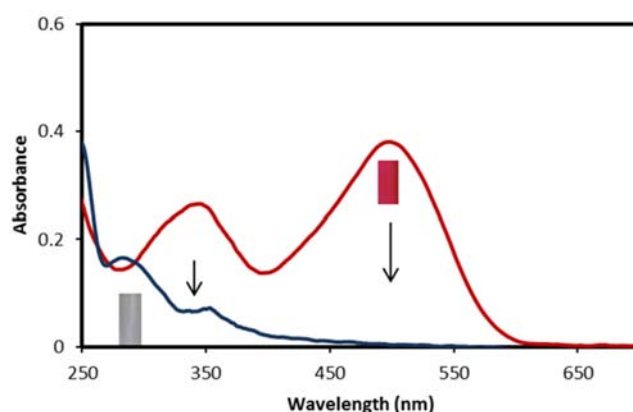


**Fig. 10.** The UV-Vis spectra of CR aqueous solution in the presence of Ag/Hazelnut shell nanocomposite.

**Table 1.** Competition time for the reduction of MO and CR using NaBH<sub>4</sub> and different amounts of Ag/Hazelnut shell nanocomposite.

Sample	[Dye] (M)	[NaBH <sub>4</sub> ] (M)	Catalyst (mg)	Time
1	MO (3.0 × 10 <sup>-5</sup> )	5.3 × 10 <sup>-3</sup>	3	12:56 min
2	MO (3.0 × 10 <sup>-5</sup> )	5.3 × 10 <sup>-3</sup>	5	7:12 min
3	MO (3.0 × 10 <sup>-5</sup> )	5.3 × 10 <sup>-3</sup>	7	1:21 min
4	MO (3.0 × 10 <sup>-5</sup> )	5.3 × 10 <sup>-3</sup>	10	55 s
5	CR (1.44 × 10 <sup>-5</sup> )	5.3 × 10 <sup>-3</sup>	3	10 min
6	CR (1.44 × 10 <sup>-5</sup> )	5.3 × 10 <sup>-3</sup>	5	5:11 min
7	CR (1.44 × 10 <sup>-5</sup> )	5.3 × 10 <sup>-3</sup>	7	1:18 min
12	CR (1.44 × 10 <sup>-5</sup> )	5.3 × 10 <sup>-3</sup>	10	49 s

**Table 2.** Completion time for the reduction of 10 ppm MO and CR dyes (25 mL) using 10 mg of hazelnut shell or 10 mg of Ag NPs in the presence of 25 mL of 250 mM of NaBH<sub>4</sub>.

Catalyst	Time (min)	
	MO	CR
Ag NPs	16	17
Hazelnut shell	150 <sup>a</sup>	150 <sup>a</sup>
-	200 <sup>a</sup>	200 <sup>a</sup>

<sup>a</sup>Not completed.

[8] M. Fu, Y. Li, S. Wu, P. Lu, J. Liu, F. Dong, *Appl. Surf. Sci.* 258 (2011) 1587-1591.  
 [9] M. Nasrollahzadeh, M. Atarod, S.M. Sajadi, *Appl. Surf. Sci.* 364 (2016) 636-644.  
 [10] M. Atarod, M. Nasrollahzadeh, S.M. Sajadi, *J. Colloid Interf. Sci.* 462 (2016) 272- 279.

[11] B. Khodadadi, *J. Sol-Gel Sci. Technol.* 80 (2016) 793-801.  
 [12] B. Khodadadi, M. Bordbar, M. Nasrollahzadeh, *J. Colloid Interf. Sci.* 490 (2017) 1-10.  
 [13] A. Rostami-Vartooni, M. Nasrollahzadeh, M. Alizadeh, *J. Colloid Interf. Sci.* 470 (2016) 268-275.  
 [14] B. Khodadadi, *Iran. J. Catal.* 6 (2016) 305-311.  
 [15] K. Afshinnia, M. Sikder, B. Cai, M. Baalousha, *J. Colloid Interf. Sci.* 490 (2017) 478-487.  
 [16] M. Zargar, A. Abdul Hamid, F. Abu Bakar, M.N. Shamsudin, K. Shameli, F. Jahanshiri, F. Farahani, *Molecules* 16 (2011) 6667-6676.  
 [17] H. Faghihian, A. Bahrani-fard, *Iran. J. Catal.* 1 (2011) 45-50.  
 [18] A. Nezamzadeh-Ejhih, M. Khorsandi, *Iran. J. Catal.* 1 (2011) 99-104.  
 [19] S. Aghabeygi, R.K. Kojoori, H. Vakili Azad, *Iran. J. Catal.* 6, 2016, 275-279.  
 [20] O.M. Kockar, O. Onay, A.E. Putun, E. Putun, *Energ. Source* 22 (2000) 913-924.

- [21] V.I. Parvulescu, B. Cojocaru, V. Parvulescu, R. Richards, Z. Li, C. Cadigan, P. Granger, *J. Catal.* 272 (2010) 92-100.
- [22] Y.L.N. Murthy, T. KondalaRao, I.V. Kasiviswanath, R. Singh, *J. Magn. Mater.* 322 (2010) 2071-2074.
- [23] G. Xin-ling, S. Zheng-tao, *Appl. Chem. Ind.* 34 (2005) 615-617.
- [24] V.K. Sharma, R.A. Yngard, Y. Lin, *Adv. Colloid Interf. Sci.* 145 (2009) 83-96.
- [25] S.S. Shankar, A. Rai, A. Ahmad, M. Sastry, *J. Colloid Interf. Sci.* 275 (2004) 496-502.
- [26] M. Atarod, M. Nasrollahzadeh, S.M. Sajadi, *J. Colloid Interf. Sci.* 462 (2016) 272-279.
- [27] K.N. Thakkar, S.S. Mhatre, R.Y. Parikh, *Nanomed. Nanotechnol. Biol. Med.* 6 (2010) 257-262.
- [28] M. Nasrollahzadeh, S. M. Sajadi, A. Hatamifard, *Appl. Catal.* 191 (2016) 209-227.
- [29] M. Bordbar, Z. Sharifi-Zarchi, B. Khodadadi, *J. Sol-Gel Sci. Technol.* 81 (2017) 724-733.
- [30] M. Nasrollahzadeh, *New J. Chem.* 38 (2014) 5544-5550.
- [31] M. Atarod, M. Nasrollahzadeh, S. M. Sajadi, *J. Colloid Interf. Sci.* 465 (2016) 249-258.
- [32] M. Atarod, M. Nasrollahzadeh, S. M. Sajadi, *RSC Adv.* 5 (2015) 91532-91543.
- [33] M. Nasrollahzadeh, S. M. Sajadi, *J. Colloid Interf. Sci.* 465 (2016) 121-127.
- [34] R. Sankar, A. Karthik, A. Prabu, S. Karthik, K. S. Shivashangari, V. Ravikumar, *Colloid Surf. B.* 108 (2013) 80-84.
- [35] A. Ocana-Fuentes, E. Arranz-Gutierrez, F.J. Senorans, G. Reglero, *Food Chem. Toxicol.* 48 (2010) 1568-1575.
- [36] S. Ceker, G. Agar, G. Nardemir, M. Anar, H.E. Kizil, L. Alpsoy, *J. Essent. Oil Bear. Pl.* 15 (2012) 997-1005.
- [37] H. Yang, R. Yan, H. Chen, D.H. Lee, C. Zheng, *Fuel* 86 (2007) 1781-1788.
- [38] I. Demiral, S.C. Kul, *J. Anal. Appl. Pyrol.* 107 (2014) 17-24.
- [39] A. Demirbas, *J. Anal. Appl. Pyrol.* 76 (2006) 285-289.
- [40] Y. Copur, C. Guler, C. Tascioglu, A. Tozluoglu, *Bioresource Technol.* 99 (2008) 7402-7406.
- [41] X. Yang, H. Zhong, Y. Zhu, H. Jiang, J. Shen, J. Huang, C. Li, *J. Mater. Chem. A* 2 (2014) 9040-9047.
- [42] K. Das, D. Ray, N. R. Bandyopadhyay, S. Sengupta, *J. Polym. Environ.* 18 (2010) 355-363.
- [43] H. Zhao, J.H. Kwak, Z.C. Zhang, H. M. Brown, B.W. Arey, J.E. Holladay, *Carbohydr. Polym.* 68 (2007) 235-241.
- [44] B. Khodadadi, M. Bordbar, M. Nasrollahzadeh, *J. Colloid Interf. Sci.* 493 (2017) 58-93.
- [45] Y. Zheng, A. Wang, *J. Mater. Chem.* 22 (2012) 16552-16559.